Available online at www.sciencedirect.com
ScienceDirect
Catalysis Today 117 (2006) 37–45
CATALYSIS TODAY
www.elsevier.com/locate/cattod

The nature of the active site for vinyl acetate synthesis over Pd–Au

M.S. Chen, K. Luo, T. Wei, Z. Yan, D. Kumar, C.-W. Yi, D.W. Goodman *

Department of Chemistry, Texas A&M University, P.O. Box 30012, College Station, TX 77842-3012, United States

Available online 16 June 2006

Abstract

The surface composition of a Pd–Au alloy was determined using low energy ion scattering spectroscopy (LEISS). A stable surface composition was found between 700 and 1000 K with substantial enrichment in Au compared to the bulk. Infrared reflection absorption spectroscopy (IRAS) and temperature programmed desorption (TPD) were used to investigate the surface adsorption sites and ensembles. The isolated Pd sites, $PdAu_6$ for Pd–Au on Mo(1 1 0) and for Pd/Au(1 1 1), and $PdAu_4$ for Pd/Au(1 0 0), were observed by controlling the Pd amount and the annealing temperature. Acetoxylation of ethylene to vinyl acetate (VA) was used to investigate the mechanism of the promotional effect of Au in a Pd–Au alloy catalyst. The enhanced rates of VA formation for low Pd coverages relative to high Pd coverages on Au single crystal surfaces demonstrate that the critical reaction site for VA synthesis consists of two, non-contiguous, suitably spaced Pd monomers. The results show that the role of Au is to isolate single Pd sites that facilitate the coupling of critical surface species to product while inhibiting the formation of undesirable reaction by-products.

Keywords: Bimetal; Palladium; Gold; Active ensemble; Vinyl acetate; Acetic acid; Ethylene

1. Introduction

Bimetallic catalysts have attracted extensive attention because of their markedly different properties from either of the constituent metals, and enhanced catalytic stabilities, activities, and/or selectivities [1]. Such research can be dated to the late 1940's with efforts to establish a direct link between electronic and catalytic properties [2]. The concepts of ''ensemble'' and ''electron'' effects were widely used to describe the origin of the enhanced activity and/or selectivity of bimetallic catalysts. Pd–Au bimetals are used as catalysts for a number of applications [3–6] including hydrogen fuel cells [7] and pollution control [8]. The addition of Au to Pd can significantly enhance its overall catalytic activity, selectivity and stability. Fig. 1 shows an example of the enhancement of catalytic activity for the oxidation of hydrogen over Pd–Au, i.e., almost two orders of magnitude increase for $Pd_{0.3}Au_{0.7}$ compared with Pd [9].

Surface composition is a key to understanding the role of alloying in mixed-metal catalysts. In this article, a planar model surface of Pd–Au/Mo(1 1 0) was prepared and used to investigate the surface composition and adsorption sites of a Pd–Au mixture. A combination of X-ray photoelectron spectroscopy (XPS) and low-energy ion scattering spectroscopy (LEISS) was used to investigate the surface concentration. Infrared reflection absorption spectroscopy (IRAS) and temperature programmed desorption (TPD) using CO as a probe molecule were used to elucidate the surface adsorption sites as well as the surface ensembles. Acetoxylation of ethylene to vinyl acetate (VA) was selected as a probe reaction of Pd–Au bimetallic surfaces. Acetoxylation of ethylene on Pd–Au bimetallic silica-supported catalysts promoted with potassium acetate (KOAc) is a well-established commercial route for the synthesis of VA [3,5,10–18].

$$CH_3COOH + C_2H_4 + 0.5O_2 \rightarrow CH_3COOCHCH_2 + H_2O$$

Although this process is a mature industrial reaction, the nature of the key reaction intermediates, mechanism and active ensemble, as well as the role of Au are still unresolved questions. A critical ensemble consisting of several Pd atoms has been suggested as the reactive site for VA synthesis [19]. We have found that the rate of VA formation is significantly enhanced on Pd/Au(1 0 0) compared with Pd/Au(1 1 1), implying that the critical reaction site for VA synthesis consists of two, noncontiguous, suitably spaced Pd monomers. This structure–activity relation provides insights into the elementary

* Corresponding author. Tel.: +1 979 845 6822; fax: +1 979 845 0214.
E-mail address: Goodman@mail.chem.tamu.edu (D.W. Goodman).

0920-5861/$ – see front matter © 2006 Elsevier B.V. All rights reserved.
doi:10.1016/j.cattod.2006.05.001

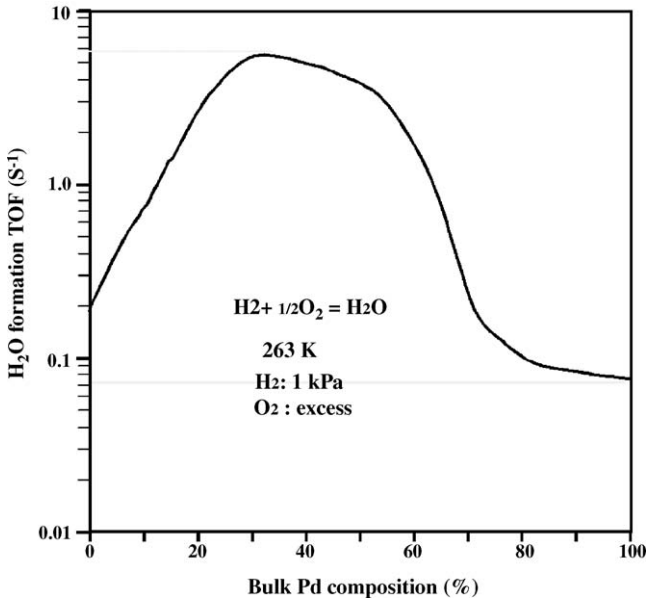

Fig. 1. H_2O formation rate for H_2 oxidation on Pd–Au alloy as a function of Pd composition. The rate was calculated on a per Pd basis using the bulk Pd ratio. The original data were obtained from Ref. [9].

steps involved in the oxidative coupling of ethylene and acetic acid to form VA, and shows that the promotional role of Au is to isolate Pd monomer sites, thereby preventing undesirable pathways to CO, CO_2 and surface carbon.

2. Experimental

The experiments were carried out in five ultrahigh vacuum (UHV) chambers equipped with XPS/LEISS [20], IRAS [20], high-resolution electron energy loss spectroscopy (HREELS) [21,22], or an XPS coupled to an elevated-pressure reactor [18,23]. Each chamber was also equipped with basic surface science techniques, Auger electron spectroscopy (AES), low-energy electron diffraction (LEED) and a quadrupole mass spectrometer. The surface composition and adsorption sites were characterized on Pd–Au/Mo(1 1 0) using the XPS/LEISS and/or the IRAS chamber. The Mo(1 1 0) sample was cleaned by repeated cycles of oxidation at 1200 K followed by a flash to 2100–2200 K, and characterized using AES and LEED. Pd and Au were evaporated from a Pd or Au wire wrapped around a Ta filament that was heated resistively. Pd and Au coverages were calibrated using TPD and AES. The coverage is reported in monolayers (ML) with respect to the top layer atom density on the Mo(1 1 0) surface [20].

The VA synthesis experiments were carried out in a combined elevated-pressure reactor-UHV XPS chamber with a base pressure of 5×10^{-10} Torr [18,23]. The Au single crystal samples, Au(1 0 0) and Au(1 1 1), were attached via tantalum supporting wires for resistive heating, and were cleaned by argon sputtering followed by annealing at 950 K. The surface cleanness was verified with AES. The substrate temperature was measured via a (W/5 wt.%Re)/(W/26 wt.%Re) thermocouple attached to the back sample surface. Pd was evaporated from a tantalum filament source onto the Au samples following by subsequent annealing in UHV. The Pd coverage was estimated from the Pd/Au AES ratio; an AES breakpoint corresponding to a monolayer was observed in a plot of Pd/Au ratio versus deposition time for Pd on Au(1 0 0) and Au(1 1 1) at or below 200 K. The Pd coverage is reported in monolayers (ML) with respect to the top layer Au atom density in Au(1 0 0) and Au(1 1 1), respectively.

After preparation and characterization in the UHV chamber, the Pd/Au sample was transferred *in situ* into the reaction chamber through a double-stage, differentially pumped Teflon sliding seal. Glacial acetic acid (CH_3COOH) was further purified by triple distillation; research-grade ethylene (C_2H_4) and ultra-high purity O_2 were used as received. A CH_3COOH:-C_2H_4:O_2 (2:4:1) mixture with a total pressure of 14 Torr was used for the kinetic studies. The vinyl acetate product was analyzed by gas chromatography using a flame ionization detector (FID).

CO adsorption was performed in the low-temperature IRAS chamber with a base pressure of $\sim 10^{-10}$ Torr. Acetic acid and ethylene adsorptions were performed in the HREELS chamber with a base pressure of $\sim 2 \times 10^{-10}$ Torr [24].

3. Results and discussion

3.1. The surface composition of Pd–Au

LEISS was used to determine the surface composition of the Pd–Au alloy surfaces [20]. Fig. 2A shows the LEISS spectra of 5 ML Pd/5 ML Au/Mo(1 1 0) as a function of annealing temperature. Following deposition of 5 ML Au onto Mo(1 1 0) at 300 K, the Au LEISS feature appears at 1.03 keV whereas no Mo feature is observed at 0.94 keV, implying that Au completely covers the substrate Mo surface. After Pd deposition onto 5 ML Au/Mo(1 1 0), the Pd LEISS feature appears at 0.97 keV, while concurrently the Au feature is significantly reduced. A Au LEISS feature was still apparent after deposition of 5 ML Pd suggesting that Pd–Au inter-diffusion and/or alloying occurs during Pd deposition onto Au at room temperature, consistent with previous observations [25]. Upon annealing to 500 K, the Pd peak intensity gradually decreased with a corresponding increase in the Au peak intensity. At elevated annealing temperatures, Au–Pd inter-diffusion is clearly apparent in the series of LEISS spectra of Fig. 2A. With further annealing at 1000 K, the Au and Pd LEISS peak intensities change very little.

The resulted surface concentrations as a function of annealing temperature for the 5 ML Pd–5 ML Au/Mo(1 1 0) are shown in Fig. 2B. For a 5 ML Pd/5 ML Au surface, the surface Au concentration gradually increases from ~4 to 80% with an increase in anneal temperature to 700 K. Between 700 and 1000 K the surface compositions of Pd and Au, $Au_{0.8}Pd_{0.2}$, remain constant. Reversing the deposition sequence, i.e., 5 ML Au/5 ML Pd, the surface Au concentration gradually decreases from ~96 to ~80% with an anneal to 700 K, then remains constant from 700 to 1000 K. These results show that 5 ML

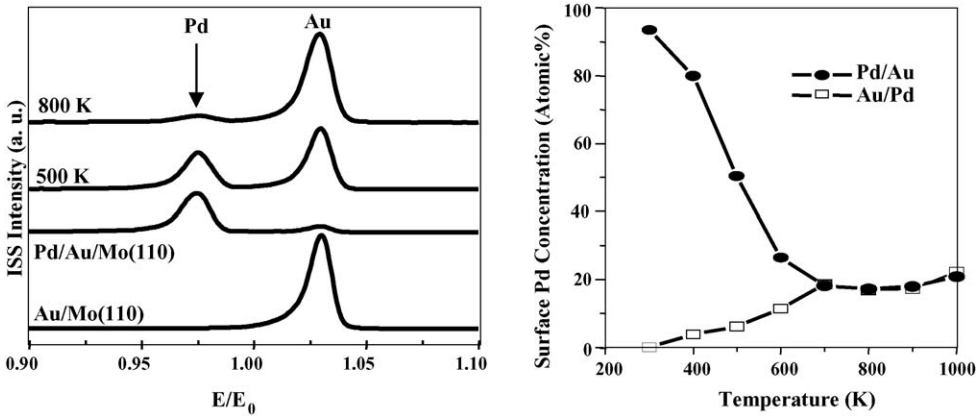

Fig. 2. Left panel: LEISS spectra of 5 ML Pd/5 ML Au/Mo(1 1 0) as a function of annealing temperature. LEISS spectra were collected at 300 K after the sample was annealed to the specified temperature. Right panel: surface concentration of Au and Pd of 5 ML Pd/5 ML Au/Mo(1 1 0) as a function of annealing temperature. The sample was annealed at each temperature for 20 min.

Pd–5 ML Au/Mo(1 1 0) form a stable surface alloy of $Pd_{0.2}Au_{0.8}$ independent of the deposition sequences. The significant enrichment of Au on the surface is a consequence of surface free energy minimization, i.e., the surface free energy for Au is 1.626 J/m^2, much lower than the corresponding value for Pd, 2.043 J/m^2 [26,27].

To further investigate the surface concentration of Pd–Au/Mo(1 1 0), experiments were carried out on various ratios of Pd/Au maintaining a constant total thickness of 10 ML. The surface (open square) versus bulk concentration (filled circle) phase diagram is plotted as a function of the Pd/Au ratio in Fig. 3. The Pd–Au/Mo(1 1 0) samples were annealed at 800 K for 20 min., and the surface composition determined by LEISS at 300 K. The results show that the surface Au composition is significantly higher than that of the bulk, and that the film results compare very favorably with previous results (open circle) obtained using bulk Pd–Au alloys [28]. The similar surface compositions between the supported Pd–Au/Mo(1 1 0) and Pd–Au alloys confirm the efficacy of the thin-film methodology used in the current studies.

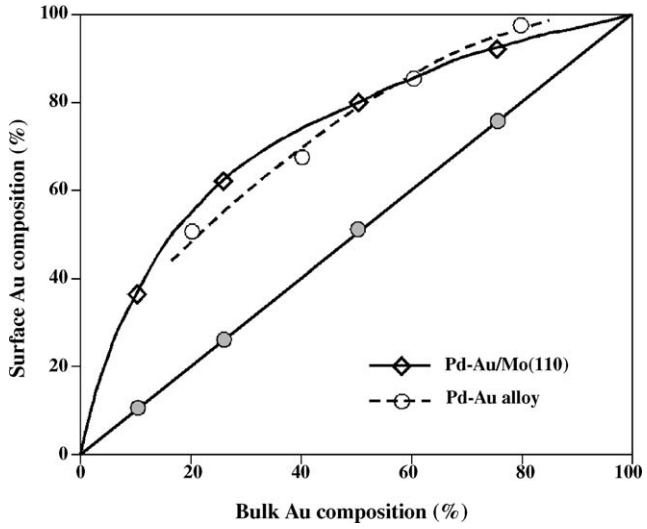

Fig. 3. Surface concentration of various Pd–Au alloys on Mo(1 1 0) measured by LEISS compared to the corresponding bulk concentration. The sample was annealed at 800 K for 20 min. Results from Pd–Au alloy were displayed together for comparison [28].

3.2. Defining the surface adsorption sites

IRAS was carried out with CO as a probe molecule in order to determine the structure of Pd–Au surface ensembles [20,22,29–33]. CO adsorbed on Pd(1 1 1) and Pd(1 0 0) surfaces have been addressed in previous work from our group [29–31]. On Pd(1 1 1) surface, the adsorption sites were found to shift from tri-hollow sites to bridge sites, then to atop and tri-hollow sites with increasing CO coverage, as shown in Fig. 4 (a–c) [29,30]. These adsorption site assignments and their CO coverage relationship was first proposed by Yates et al. [34] using TPD and LEED. On Pd(1 0 0), CO was found to adsorb only at bridging sites over the entire coverage range [31]. A spectrum of CO on Pd(1 0 0) with saturate CO coverage is shown in Fig. 4(d). For model oxide supported Pd particles, three CO vibrational features, atop, (1 0 0) bridge sites and (1 1 1)-tri-hollow sites, are observed as shown in Fig. 4(e), consistent with Pd(1 0 0) and (1 1 1) facets being prevalent on these particles [33].

Fig. 5A shows IRAS spectra as a function of the CO exposure at 90 K onto a 5 ML Pd/5 ML Au/Mo(1 1 0) surface annealed at 600 K for 20 min. Following a relatively low exposure of CO (<0.10 L), IRAS shows mainly two stretching features at 2087 and 1940 cm^{-1}, corresponding to linearly- and bridged-bound CO on metal surfaces, respectively. These assignments are consistent with the general features of CO on Pd(1 1 1), i.e., 2110–2080 cm^{-1} for linearly bound CO, 1965–1900 cm^{-1} for two-fold bridging CO and 1900–1800 cm^{-1} for three-fold bound CO species [34,35]. These designations also agree with the assignment of Koel et al., i.e., 1910 and 2090 cm^{-1} to bridging and a-top sites bounding, respectively, for Pd/Au(1 1 1) [17]. With further CO exposure (≥0.20 L), a new feature appears at 2105 cm^{-1} and saturates at 0.5 L CO dose. The feature at 2105 cm^{-1} is assigned to atop CO on Au, since the vibrational frequency of CO on atop sites of Au fall

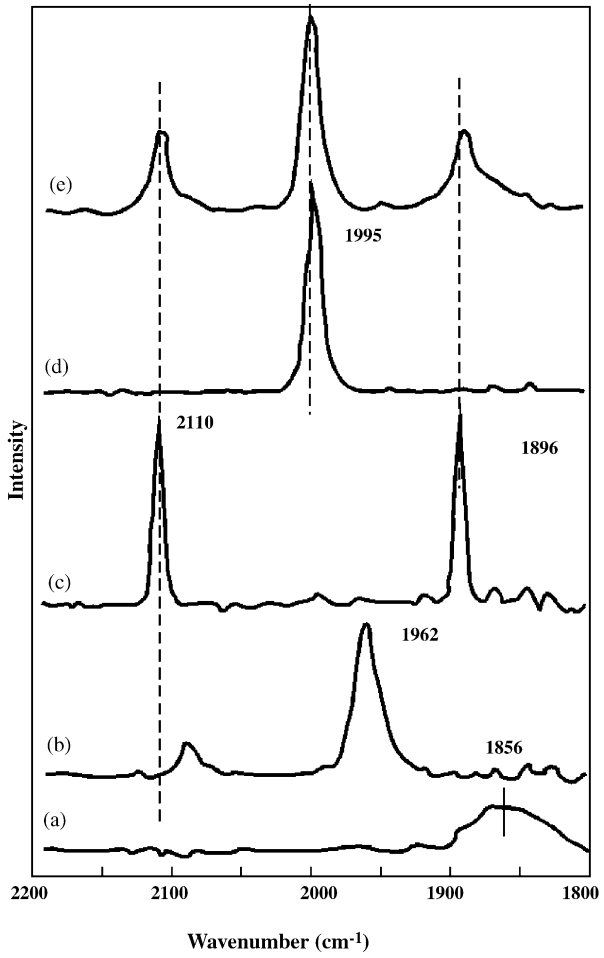

Fig. 4. IRAS spectra for CO adsorption on: (a–c) Pd(1 1 1) at 500, 200 and 100 K in 1×10^{-6} Torr CO; (d) Pd(1 0 0) with saturated CO coverage; (e) Pd/SiO_2 with saturated CO coverage. The original data were obtained from Ref. [29].

within the range 2120–2100 cm^{-1} [36]. In addition this feature disappears below 200 K, a much lower temperature than for atop CO on Pd [20]. Fig. 5B shows CO on a 5 ML Pd/5 ML Au/Mo(1 1 0) annealed at 800 K for 20 min. Only a feature at 2087 cm^{-1} corresponding to CO atop on Pd appears at a CO coverage <0.10 L; with increasing CO exposure, a second feature at 2112 cm^{-1} corresponding to atop CO on Au [20]. It is noteworthy that multi-fold CO vibrational features were not observed on this surface, indicating that the surface Pd atoms were isolated by Au atoms, e.g. formation of $PdAu_6$. Such isolated Pd ensembles were previously observed using STM and CO adsorption by Behm et al. [37], and is consistent with the LEISS results of Fig. 2, i.e., the surface concentration of Pd is reduced to ~18% upon annealing a 5 ML Pd–5 ML Au/Mo(1 1 0) surface at 800 K for 20 min.

CO-TPD was used to further characterize the surface adsorption sites on Pd–Au/Mo(1 1 0), as well as on Pd/Mo(1 1 0) [20,38]. The results were shown in Fig. 6. On the 5 ML Pd–5 ML Au/(1 1 0) alloy surface, there are two TPD peaks, ~100 and 300 K corresponding to CO atop on Au and Pd; whereas on the Pd/Mo(1 1 0) surface, higher temperature features between 400 and 500 K corresponding to CO adsorbed on the bridge and tri-hollow sites were observed [20,38]. The absence of CO desorption features above 350 K on the Pd–Au alloy surface indicates no multi-fold Pd adsorption sites on the surface, consistent with IRAS (Fig. 5) and LEISS (Fig. 2) results that all surface Pd atoms were isolated by Au atoms forming Pd monomer, $PdAu_6$.

3.3. Vinyl acetate synthesis over Pd/Au(1 0 0) and Pd/Au(1 1 1)

To investigate the promotional effect of Au in a Pd–Au alloy catalyst, acetoxylation of ethylene to vinyl acetate (VA) was used as a probe reaction. The VA synthesis experiments were

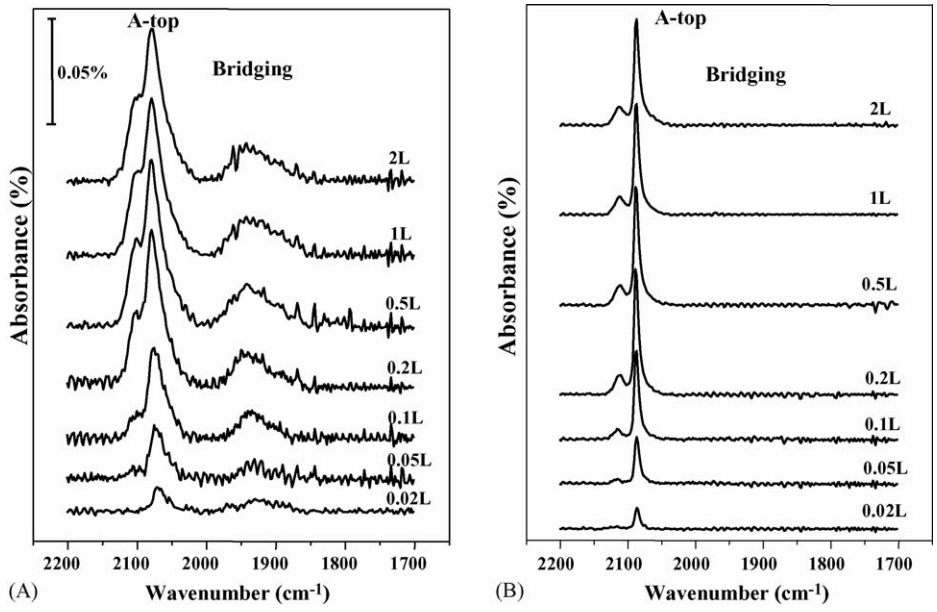

Fig. 5. IRAS of CO on 5 ML Pd/5 ML Au/Mo(1 1 0) as a function of CO exposure. (A) Annealed at 600 K for 20 min, (B) annealed at 800 K for 20 min.

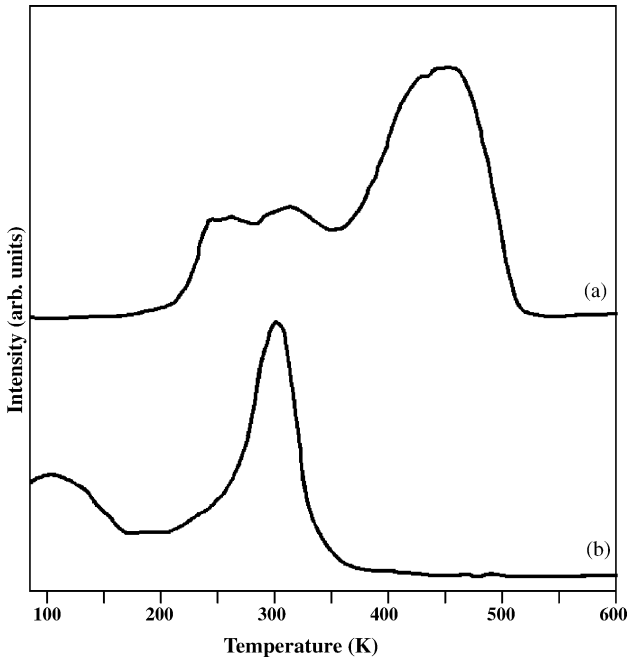

Fig. 6. TPD of CO on: (a) 10 ML Pd/Mo(1 1 0), and (b) 5 ML Pd/5 ML Au/Mo(1 1 0) annealed at 800 K for 20 min.

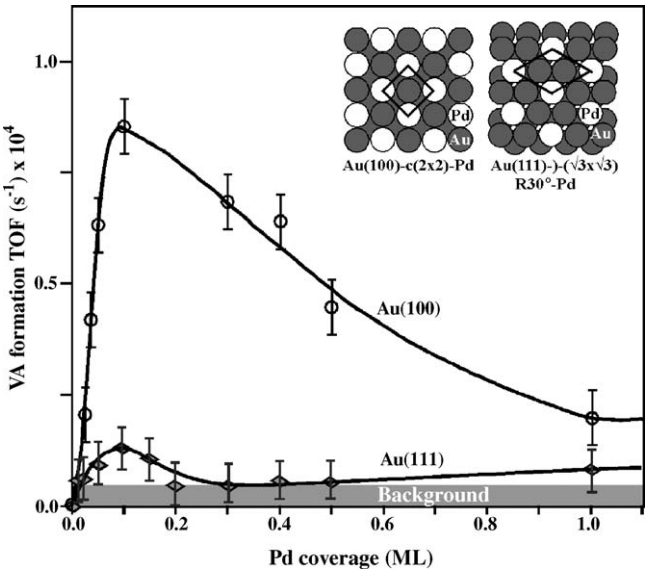

Fig. 7. Vinyl acetate (VA) formation rates as a function of Pd coverage. The TOF's are computed with respect to the (1 × 1) surface unit. The VA synthesis was carried out at 453 K, with acetic acid, ethylene and O_2 pressures of 4, 8 and 2 Torr, respectively. Total reaction time is 3 h. The error bars are based on background rate data. Inserts show the structures for Au(1 0 0)-c(2 × 2)-Pd and Au(1 1 1)-$(\sqrt{3} \times \sqrt{3})$R30°-Pd, where the maximum number of surface Pd monomers occur for the Pd/Au(1 0 0) and Pd/Au(1 1 1) surfaces, respectively.

carried out on Pd/Au(1 0 0) and Pd/Au(1 1 1) at 453 K [22]. Pd atoms were evaporated onto clean Au surfaces from a filament source followed by an anneal at 550 K. The rate of VA formation, expressed as a turnover frequency (TOF), or the number of VA molecules produced per surface atom site per second, rises to a maximum as the Pd coverage is lowered to approximately 0.1 monolayer (ML = one Pd per Au surface atom), then decreases sharply with a further decrease in the Pd coverage below 0.1 ML, as shown in Fig. 7. The TOF's for Pd/Au(1 0 0) are significantly higher than the corresponding values for Pd/Au(1 1 1) over the entire Pd coverage range.

The formation of surface Pd monomers for Pd/Au(1 0 0) and Pd/Au(1 1 1) were confirmed by adsorption of CO, accompanied by IRAS. Intense CO vibrational features between 1900 and 2000 cm^{-1} corresponding to CO adsorption on two-fold bridging and/or three-fold hollow sites [29–33,39,40] were observed for multilayer Pd on Au(1 0 0) and Au(1 1 1) deposited at or below room temperature as shown in Fig. 8. These data are evidence for the formation of Pd overlayers on Au(1 1 1) or Au(1 0 0), and are consistent with previous studies [41,42]. Upon annealing Pd/Au(1 0 0) or Pd/Au(1 1 1) at higher than 600 K, the CO features in the IRAS data corresponding to bridging and/or three-fold hollow sites disappear and the intensity of the features corresponding to atop sites between 2125 and 2080 cm^{-1} increase significantly. These results demonstrate that continuous surface Pd ensembles are broken up upon annealing to form isolated Pd sites or monomers, i.e., Au_4Pd on Au(1 0 0) and Au_6Pd on Au(1 1 1) (see the schematic in Fig. 9). The formation of surface Pd monomers on Au(1 1 1) has been observed previously by STM [37]. Furthermore, after heating to 500 K a significant decrease in the surface Pd coverage on Au(1 1 1) was observed by LEISS [41]. A maximum in the density of Pd monomers should occur at 1/2 ML Pd on Au(1 0 0) and at 1/3 ML Pd on Au(1 1 1), coverages that correspond to the Au(1 0 0)-c(2 × 2)-Pd and Au(1 1 1)-$(\sqrt{3} \times \sqrt{3})$R30°-Pd structures, respectively (see

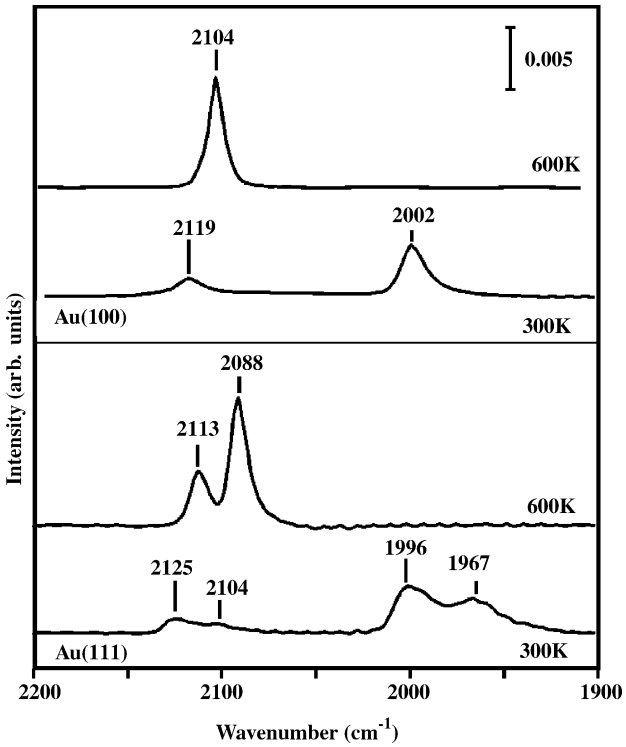

Fig. 8. IRAS spectra for CO adsorption at 90 K on 4 ML Pd/Au(1 0 0) and 4 ML Pd/Au(1 1 1); Pd was deposited at 90 K with a subsequent anneal at 300 and 600 K, each for of 10 min.

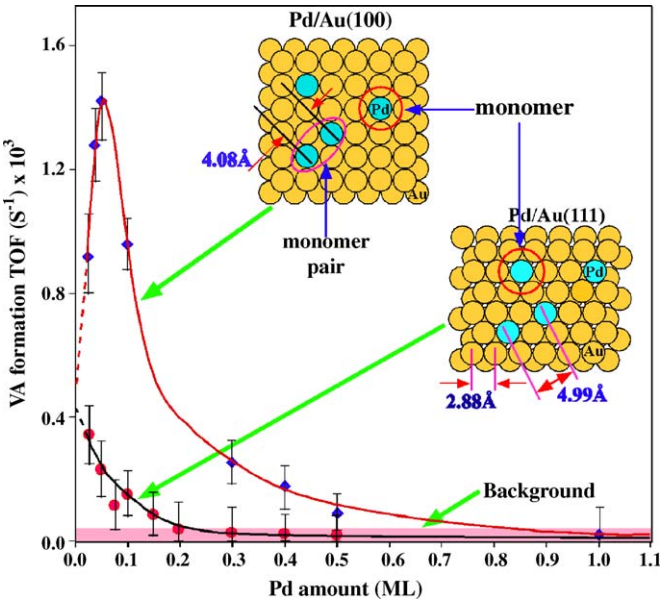

Fig. 9. Vinyl acetate (VA) formation rates as a function of Pd coverage. The TOF's are computed with respect to the Pd atom concentration. The VA synthesis was carried out at 453 K, with acetic acid, ethylene and O_2 pressures of 4, 8 and 2 Torr, respectively. Total reaction time is 3 h. The error bars are based on background rate data. The inserts show Pd monomers and monomer pairs on the Au(1 0 0) and Au(1 1 1).

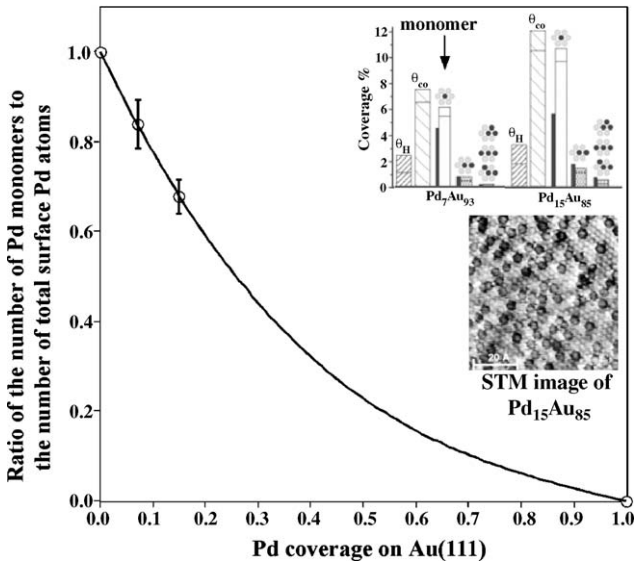

Fig. 10. The ratio of the number of Pd monomers to the number of total surface Pd atoms as a function of Pd coverage. The original data were obtained from Ref. [37].

inserts of Fig. 7). However, no such well-ordered surface structures were observed, likely because Pd and Au are completely miscible over the entire range of compositions, i.e., bulk diffusion of Pd occurs. The much lower surface energy of Au also favors surface enrichment by Au [43]. A surface Pd coverage of 0.2 ML was observed for a Pd–Au bimetal films (1:1 atomic ratio) on Mo(1 1 0) leading to mainly Pd monomers [20].The surface coverage of Pd deposited on Au(1 0 0) or Au(1 1 1) following an anneal increases continuously with increasing Pd coverage as evidenced by the concomitant increase in the ratio of Pd relative to Au by AES or LEISS [28,43]. If each surface Pd atom can serve as an active site for VA synthesis, then the overall catalytic rate of VA formation should increase steadily with an increase in the Pd coverage up to one monolayer. However the data displayed in Fig. 7 for Pd/Au(1 0 0) and Pd/Au(1 1 1) show a decidedly different behavior, namely, an increase in the VA TOF with an increase in the Pd coverage from 0 to 0.1 ML followed by a gradual decline in the rate from 0.1 to 1.0 ML, approaching the rate observed for Pd(1 0 0) at 1.0 ML. These results strongly implicate isolated Pd sites or monomers as catalytically active sites on Au(1 0 0) and Au(1 1 1) for VA synthesis, as seen from the density of the surface isolated Pd as a function of Pd coverage measured by STM in Fig. 10. Note that in VA synthesis reaction conditions some subsurface Pd atoms may surface segregate as evidenced by our XPS and LEISS results. Similar results have been reported with O_2 and/or H_2 [44,45].

Because the VA synthesis rate on a Au-only surface is extremely low compared to the rate on a Pd–Au surface, it is appropriate to express the VA formation rate for Pd/Au with respect to the atomic fraction of Pd at the surface, as shown in Fig. 9. The rate per Pd (TOF) on the Au(1 0 0) surface becomes significantly higher as the Pd coverage is reduced, until a maximum is reached at a Pd coverage of ~0.07 ML. The corresponding TOF's for Pd on Au(1 1 1) rise steadily as the Pd coverage is decreased, and at all Pd coverages the VA rate for Pd on Au(1 1 1) is significantly lower compared to the rate for the corresponding Pd coverage on Au(1 0 0). Nevertheless the data in Figs. 7 and 9 support isolated Pd sites being more active for VA synthesis compared to surface ensembles containing contiguous Pd atoms. As seen in Fig. 10, the ratio of the number of the surface isolated Pd to that of the all surface Pd atoms decreases with increasing Pd coverage [37].

For Pd/Au(1 1 1) the monotonic increase in the TOF's for VA formation in Fig. 9 with decreasing Pd coverage is consistent with isolated Pd atoms being active catalytic sites. On the other hand, the sharp maximum in the data for Pd/Au(1 0 0) in Fig. 9 at a Pd coverage of ~0.07 ML suggests that a pair of non-contiguous Pd sites, i.e., a pair of Pd monomers (as indicated in Fig. 9), is much more effective for VA formation than a single, isolated Pd site. The differences in VA synthesis activities between Pd/Au(1 0 0) and Pd/Au(1 1 1) then merit discussion. The reaction mechanism for VA synthesis remains uncertain, however, two pathways have been proposed in the literature: (i) adsorption and subsequent activation of ethylene to form a vinyl species that then couples with a coadsorbed acetate species to form VA; [10] and (ii) adsorbed ethylene reacts with an adsorbed acetate nucleophile to form an ethyl-acetate-like intermediate which then undergoes a β-H elimination to form VA [11]. Scavenging of the hydrogen with oxygen occurs to complete the reaction.

Both mechanisms assume that the coupling of surface ethylene species and acetate to form VA is the rate-limiting step [10,11,13]. An illustration of the coupling reaction between a surface ethylene and acetate species utilizing a pair of Pd sites

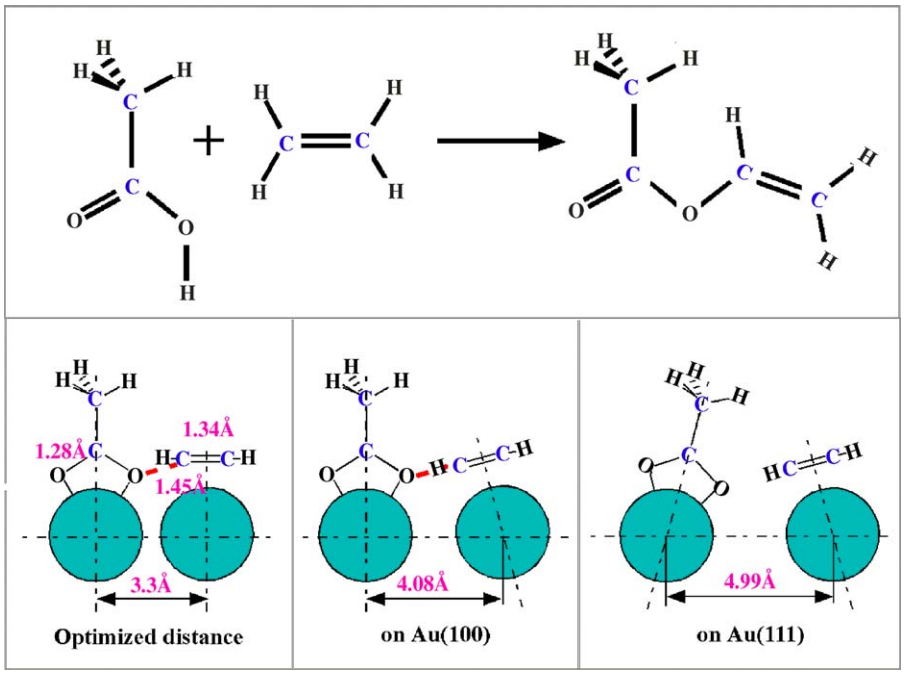

Fig. 11. Schematic for VA synthesis from acetic acid and ethylene. The optimized distance between the two active centers for the coupling of surface ethylene and acetate species to form VA is 3.3 Å. With lateral displacement, coupling of an ethylene and acetate species on a Pd monomer pair is possible on the Au(1 0 0), but unlikely on the Au(1 1 1).

is shown in Fig. 11. This rate-limiting step being the insertion of ethylene into an adsorbed acetate species and subsequent β-H elimination to form VA is supported by recent new experimental results from Tysoes group [46]. The bidentate acetate species and the π-bonding of ethylene on the Pd monomers was deduced using HREELS as shown in Fig. 12. The appearance of loss peaks at ∼1420 and 2950 cm^{-1} and the absence of a peak at ∼1700 cm^{-1} are evidence of a bidentate acetate surface species on surfaces with isolated and contiguous Pd sites (Fig. 12A). For ethylene adsorption, only π bonding of an ethylene species was observed on a surface with only isolated Pd sites, whereas di-σ bonding ethylene and ethylidyne species were found on a surface with continuous Pd sites. The detail assignments of surface species for acetic acid [47] and ethylene [48–50] adsorption have been discussed previously.

Using bond lengths of the parent molecules, the optimum spacing between the two active sites to couple the reacting species is approximately 3.3 Å. On the Au(1 0 0) surface, the spacing between two neighboring Pd monomers is 4.08 Å, acceptably close for coupling of the adsorbed surface species. On the other hand, on the Au(1 1 1) surface, the nearest distance between two neighboring Pd monomers is 5.0 Å, much larger than the ideal 3.3 Å, yielding, as a consequence, a much lower rate of VA formation compared with Pd/Au(1 0 0). Much larger Pd ensembles have been predicted as a prerequisite for carrying out VA synthesis [19]. The data presented here show

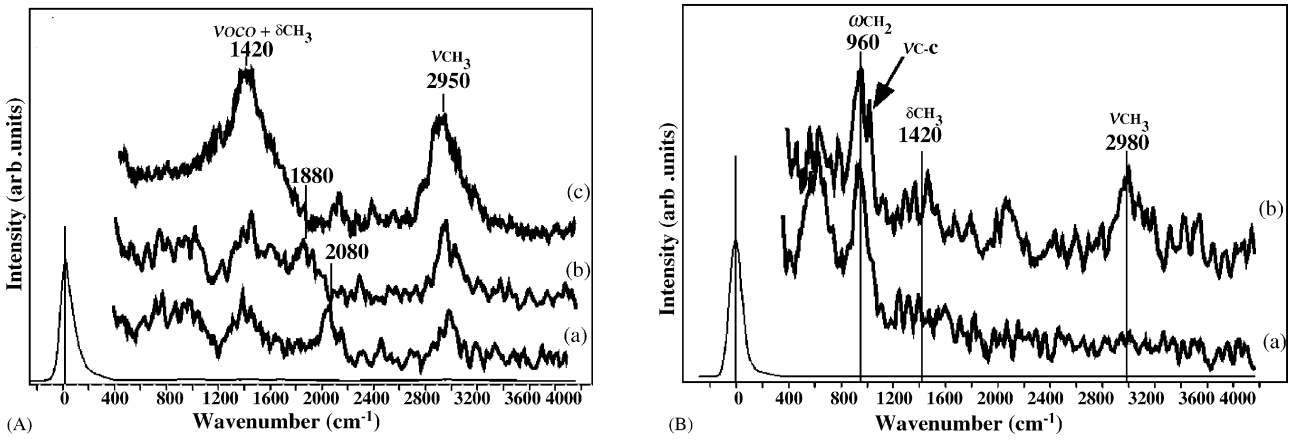

Fig. 12. HREELS spectra of: (A) acetic acid adsorption on (a) Pd/Au(1 1 1) with only isolated Pd sites, (b) Pd/Au(1 1 1) with continuous Pd sites, and (c) 1 ML Pd/Au(1 1 1) after VA synthesis reaction for 3 h. (B) Ethylene adsorption on (a) Pd/Au(1 1 1) with only isolated Pd sites, and (b) Pd/Au(1 1 1) with continuous Pd sites. Acetic acid was dosed into the chamber with a background pressure of 2×10^{-8} Torr and cooling the sample from 350 to 210 K. Ethylene was dosed into the chamber with a background pressure of 2×10^{-8} Torr, then cooling the sample from 300 to 170 K.

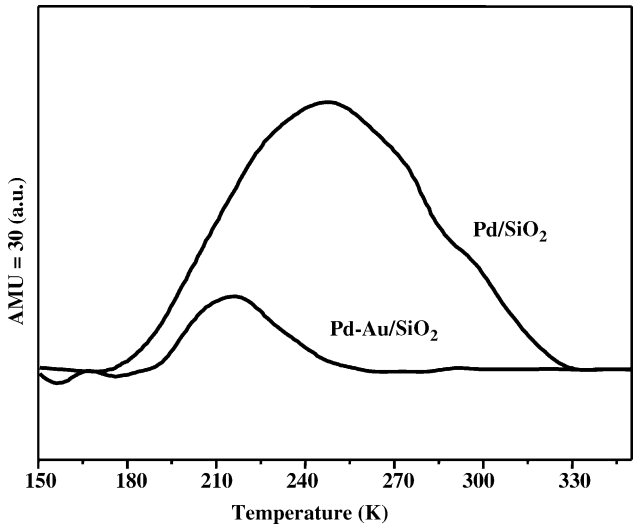

Fig. 13. TPD of ethylene (C_2D_4) from supported Pd and Pd–Au alloy clusters.

not only that larger Pd ensembles are not required, but indeed that larger ensembles containing contiguous Pd atoms are much less efficient than a properly spaced pair of Pd monomers.

The significantly higher VA formation rate at Pd monomer sites can be explained by alloying (electronic), strain, and/or ensemble effects. With respect to an electronic effect, the chemisorptive properties of a metal overlayer on a dissimilar metal can differ dramatically from those of the parent bulk overlayer metal [51]. For example, the adsorption energies and dissociative reaction barriers of small molecules such as CO have been correlated with changes in the electronic properties of certain alloy overlayers [52]. However, for a Pd–Au alloy, the lattice strain is minimal with only a 4% lattice mismatch between a relaxed Pd overlayer and a Au(1 0 0) or Au(1 1 1) surface. Furthermore, the work functions for Au and Pd are very similar (5.3 eV versus 5.6 eV, respectively) and the electronegativities are identical (1.4). XPS core-level data imply very limited charge transfer between Pd and Au in Pd–Au alloys [41]. Altogether these data are consistent with minimal electronic and strain effects in a Pd–Au alloy. The primary explanation of choice for the unusually high activity of a Pd monomer for VA formation then is an ensemble effect, i.e., the formation of Pd monomers inhibits the formation of undesirable byproducts, e.g. CO, CO_2 and surface carbon. As shown in Fig. 6, CO TPD peak position for CO on a Pd–Au surface without continuous Pd sites is much lower than that from a Pd surface. Note that CO is a reaction intermediate or by-product in VA synthesis reaction, the strong adsorption of CO on the continuous Pd sites may poison the surface active sites thus decrease the activity. Ethylene was found to bind significantly less strongly on an isolated Pd site compared to contiguous Pd sites, as shown from the TPD of ethylene (Fig. 13) [38]. Furthermore, the surface species are different on isolated Pd and continuous Pd (Fig. 12B). The di-σ bonding ethylene and ethylidyne species formed on the surface with continuous Pd sites may further decompose into carbon species on the surface thus block and poison the surface active sites. The addition of Au to Pd significantly suppresses carbon deposition via reactant and product decomposition for high surface area supported catalysts [53,54].

4. Conclusions

The surface composition of Au–Pd alloys was investigated by LEISS on a model alloying system grown on a refractory metal single crystal surface. Surface ensembles were probed by CO adsorption using IR and TPD. Preferential surface enrichment of Au was observed. The surface Pd atoms were isolated by Au atoms forming Pd monomers upon reducing the surface Pd amount by annealing. The catalytic activity of the alloy surfaces was measured using acetoxylation of ethylene to VA. The enhanced rates of VA formation for low Pd coverages relative to high Pd coverages on Au single crystal surfaces demonstrate that the critical reaction site for VA synthesis consists of two, non-contiguous, suitably spaced Pd monomers. The role of Au is to isolate single Pd sites that facilitate the coupling of critical surface species to product while inhibiting the formation of undesirable reactions by-products.

Acknowledgements

We gratefully acknowledge the support of this work by the Department of Energy, Office of Basic Energy Sciences, Division of Chemical Sciences, and the Robert A. Welch Foundation.

References

[1] M.A.C. Nascimento, Theoretical Aspects of Heterogeneous Catalysis, vol. 8, Kluwer Academic Publishers, Dordrecht; Boston, MA, 2001.
[2] G.M. Schwab, Disc. Faraday Soc. 8 (1950) 166.
[3] E.G. Allison, G.C. Bond, Catal. Rev. 7 (1972) 233.
[4] P.N. Rylander, Catalytic Hydrogenation in Organic Synthesis, Academic Press, London, 1979.
[5] R. Abel, P. Collins, K. Eichler, I. Nicolau, D. Peters, in: G. Ertl, H. Knözinger, J. Weitkamp (Eds.), Handbook of Heterogeneous Catalysis, vol. 5, Wiley-VCH, Weinheim, 1997 , p. 2298 (chapter 4.6.5.4B).
[6] A.M. Venezia, V. La Parola, V. Nicoli, G. Deganello, J. Catal. 212 (2002) 56.
[7] D.L. Trimm, Z.I. Onsan, Catal. Rev. 43 (2001) 31.
[8] M. Bonarowska, A. Malinowski, W. Juszczyk, Z. Karpinski, Appl. Catal. B 30 (2001) 187.
[9] Y.L. Lam, J. Criado, M. Boudart, Nouveau J. Chim. 1 (1977) 461.
[10] S. Nakamura, T. Yasui, J. Catal. 17 (1970) 366.
[11] B. Samanos, P. Boutry, J. Catal. 23 (1971) 19.
[12] W.D. Provine, P.L. Mills, J.J. Lerou, Stud. Surf. Sci. Catal. 101 (1996) 191.
[13] N. Macleod, J.M. Keel, R.M. Lambert, Appl. Catal. A 261 (2004) 37.
[14] Y.F. Han, D. Kumar, D.W. Goodman, J. Catal. 230 (2005) 353.
[15] D. Stacchiola, F. Calaza, L. Burkholder, W.T. Tysoe, J. Am. Chem. Soc. 126 (2004) 15384.
[16] Y.-F. Han, D. Kumar, C. Sivadinarayana, D.W. Goodman, J. Catal. 224 (2004) 60.
[17] Y.-F. Han, J.-H. Wang, D. Kumar, Z. Yan, D.W. Goodman, J. Catal. 232 (2005) 467.
[18] D. Kumar, Y.F. Han, M.S. Chen, D.W. Goodman, Catal. Lett., 106 (2006) 1.
[19] M. Neurock, J. Catal. 216 (2003) 73.
[20] C.-W. Yi, K. Luo, T. Wei, D.W. Goodman, J. Phys. Chem. B 109 (2005) 18535.
[21] M.S. Chen, A.K. Santra, D.W. Goodman, Phys. Rev. B 69 (2004) 155404.

[22] M.S. Chen, D.W. Goodman, Science 306 (2004) 252.
[23] M.S. Chen, D. Kumar, C.-W. Yi, D.W. Goodman, Science 310 (2005) 291.
[24] M.S. Chen, A.K. Santra, D.W. Goodman, J. Phys. Chem. B 108 (2004) 17940.
[25] A. Sellidj, B.E. Koel, Phys. Rev. B 49 (1994) 8367.
[26] L.Z. Mezey, J. Giber, Japn. J. Appl. Phys. 21 (1982) 1569.
[27] R. Anton, H. Eggers, J. Veletas, Thin Solid Films 226 (1993) 39.
[28] D.G. Swartzfager, S.B. Ziemecki, M.J. Kelley, J. Vac. Sci. Technol. 19 (1981) 185.
[29] W.K. Kuhn, J. Szanyi, D.W. Goodman, Surf. Sci. 274 (1992) L611.
[30] W.K. Kuhn, J. Szanyi, D.W. Goodman, Surf. Sci. 303 (1994) 377.
[31] J. Szanyi, W.K. Kuhn, D.W. Goodman, J. Vac. Sci. Technol. A 11 (1993) 1969.
[32] D.W. Goodman, Surf. Rev. Lett. 2 (1995) 9.
[33] D.R. Rainer, M.C. Wu, D.I. Mahon, D.W. Goodman, J. Vac. Sci. Technol. A 14 (1996) 1184.
[34] X.C. Guo, J.T. Yate Jr., J. Chem. Phys. 90 (1989) 6761.
[35] E. Ozensoy, D.W. Goodman, Phys. Chem. Chem. Phys. 6 (2004) 3765.
[36] D.C. Meier, D.W. Goodman, J. Am. Chem. Soc. 126 (2004) 1892.
[37] F. Maroun, F. Ozanam, O.M. Magnussen, R.J. Behm, Science 293 (2001) 1811.
[38] K. Luo, T. Wli, C.-W. Yi, S. Axnanda, D.W. Goodman, J. Phys. Chem. B 109 (2005) 23517.
[39] C.T. Campbell, Curr. Opin. Solid State Mater Sci. 3 (1998) 439.
[40] K. Wolter, O. Seiferth, J. Libuda, H. Kuhlenbeck, M. Baumer, H.J. Freund, Surf. Sci. 404 (1998) 428.
[41] B.E. Koel, A. Sellidj, M.T. Paffett, Phys. Rev. B 46 (1992) 7846.
[42] C.J. Baddeley, C.J. Barnes, A. Wander, R.M. Ormerod, D.A. King, R.M. Lambert, Surf. Sci. 314 (1994) 1.
[43] A. Jablonski, S.H. Overbury, G.A. Somorjai, Surf. Sci. 65 (1977) 578.
[44] L. Hilaire, P. Légaré, Y. Holl, G. Maire, Surf. Sci. 103 (1981) 125.
[45] L.Z. Mezey, W. Hofer, P. Varga, J. Giber, Surf. Inter. Anal. 16 (1990) 520.
[46] D. Stacchiola, F. Calaza, L. Burkholder, A.W. Schwabacher, M. Neurock, W.T. Tysoe, Angew. Chem. Int. Ed. 44 (2005) 4572.
[47] R.D. Haley, M.S. Tikhov, R.M. Lambert, Catal. Lett. 76 (2001) 125.
[48] J.M. Heitzinger, S.C. Gebhard, B.E. Koel, J. Phys. Chem. 97 (1993) 5327.
[49] M. Sock, A. Eichler, S. Surnev, J.N. Andersen, B. Klotzer, K. Hayek, M.G. Ramse, F.P. Netzer, Surf. Sci. 545 (2003) 122.
[50] S. Azad, M. Kaltchev, D. Stacchiola, G. Wu, W.T. Tysoe, J. Phys. Chem. B. 104 (2000) 3107.
[51] J.A. Rodriguez, D.W. Goodman, Science 257 (1992) 897.
[52] B. Hammer, Y. Morikawa, J.K. Norskov, Phys. Rev. Lett. 76 (1996) 2141.
[53] Y.F. Han, D. Kumar, C. Sivadinarayana, A. Clearfield, D.W. Goodman, Catal. Lett. 94 (2004) 131.
[54] M. Bowker, C. Morgan, Catal. Lett. 98 (2004) 67.